

## 8. ADVANCE FEATURES IN THE SPAN AND SPAN/XRF GAMMA RAY AND X RAY SPECTRUM ANALYSIS SOFTWARE<sup>12</sup>



XA9848359

### 8.1. SUMMARY

This paper describes the advanced techniques, integral peak background, experimental peak shape and complex peak shape, which have been used successfully in the software packages SPAN and SPAN/XRF to process gamma ray and X ray spectra from HPGe and Si(Li) detector. Main features of SPAN and SPAN/XRF are also described. The software runs on PC and has convenient graphical capabilities and a powerful user interface.

### 8.2. INTRODUCTION

With the advance of high resolution HPGe, Ge(Li) and Si(Li) detectors,  $\gamma$  ray and X ray spectrometry has made great progress and has been widely used in many fields of pure and applied science, e.g. neutron activation analysis and X ray fluorescence analysis. The processing of  $\gamma$  ray and X ray spectrum data includes peak searching, background subtracting, multiplet resolving, and nuclide or element identification. To me, the key (important technique) is multiplet resolving, i.e., to get an accurate analytical result of photopeaks in multiplet for X ray and  $\gamma$  ray spectrum.

Now-a-days most authors in their software for nuclear spectrometry use analytical functions hereafter called peak shape functions, to fit and resolve multiplets [1, 2]. Many peak shape functions has been applied [11, 12, 13, 14], which consist of a main Gaussian function and some additive components. The Gaussian function is the simplest peak shape function, which deals with only three parameters:

$$F_i = \frac{S}{\sqrt{2\pi} * \sigma} * \exp\left(-\frac{(i-i_0)^2}{2\sigma^2}\right) \quad (1)$$

where:  $i_0$  is the center of the peak,  
 $\sigma$  is the peak width,  
 $S$  is peak area.

The additive components are used for correcting the peak shape function to emulate the experimental peak shape, for example non-symmetry, short and long tails, etc. The HYPERMET function [3] was used in quite a number of software:

$$F_i = A * \exp\left(-\frac{(i-i_0)^2}{2\sigma^2}\right) + B * \exp\left(\frac{i-i_0}{\beta}\right) * \frac{1}{2} * \operatorname{erfc}\left(\frac{i-i_0}{\sigma\sqrt{2}} + \frac{\sigma}{\beta\sqrt{2}}\right) \quad (2)$$

---

<sup>12</sup> Prepared by WANG LI-YU, China Institute of Atomic Energy, China.

in which 5 parameters need to be fitted. Some more complex functions were designed, for example Kern [4] suggested following function:

$$F_i = A * \exp\left(-\frac{(i-i_0)^2}{2\sigma^2}\right) * \left(1 + p_3 \left(\frac{(i-i_0)}{\sigma}\right)^4 + p_4 \left(\frac{(i-i_0)}{\sigma}\right)^{12}\right) + \frac{A}{\sigma} * \left(1 + \frac{1}{\left(\frac{(i-i_0)^2}{\sigma^2} + 1\right)}\right) * \left[p_2 + p_3 \exp\left(\frac{p_6(i-i_0)}{\sigma}\right)\right] \quad (3)$$

The function with more parameters to be fitted emulates the peak in experimental spectrum more closely, but the fact that more parameters have to be fitted leads to a more complicated calculation, and increases the probability of a failure. Some analytical functions were designed to fit the baseline continuum under the peak. For the cases shown in formulas (2) or (3) and additional function describing the continuum need to be fitted as well. Thus, the fitting calculation will be even more complicated. For example, suppose there are 4 peaks in a multiplet; taking above-mentioned formulas, each peak has 6 parameters, and then the continuum has 3 parameters, so ending in a total amount of 27 parameters to be fitted. It is not an easy task to calculate 27 x 27 array. Besides, the peak shape is not only depended on the detector and amplifier, but also depends on sample conditions, such as dimension, thickness, etc. Therefore only one analytical peak shape function is not suitable to describe all these conditions.

Under these circumstances, I came to the idea that why not to use directly the *experimental peak shapes* to fit multiplets. This numerical method can be used to fully resolve the problem. Under this concept, some new techniques and algorithms have been developed in the software packages SPAN and SPAN/XRF, they are:

- (1) Integral peak baseline.
- (2) Experimental peak shape.
- (3) Complex peak shape.

Due to the application of these techniques, the analysis of spectral data becomes very fast and the accuracy is satisfactory. These techniques are discussed below.

### 8.3. INTEGRAL PEAK BACKGROUND

To describe the baseline under peak correctly is the key to get an accurate net peak area. Watching a g ray or X ray spectrum, we can find the baseline levels are different before and after a peak, especially for a strong peak, see Fig.1.

It is quite evident that a straight line or a quadratic curve can not satisfactorily describe the baseline continuum. Some step functions were designed, such as arc tangent function etc.; but these functions are also not satisfactory because they lack of continuity with the "outside-peak" baseline and sometimes they are not acceptable, see Fig.2. W.Watzig [5] in 1978 designed the "integral peak background" method, with which the baseline can be directly subtracted. I improved this technique and it has been satisfactorily used in the software SPAN [6].

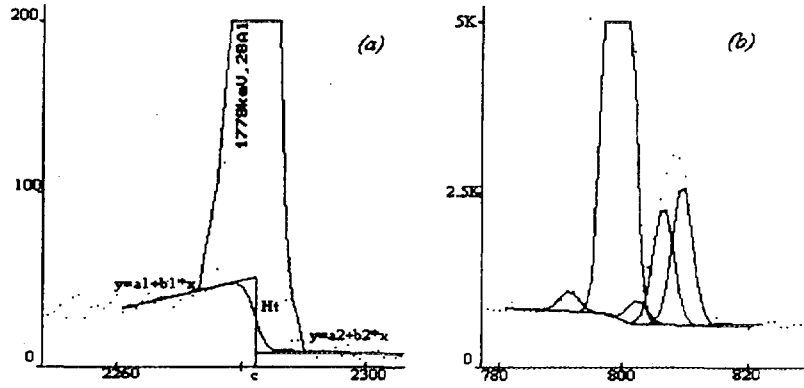


FIG 1. The integral peak background under singlet and multiplet

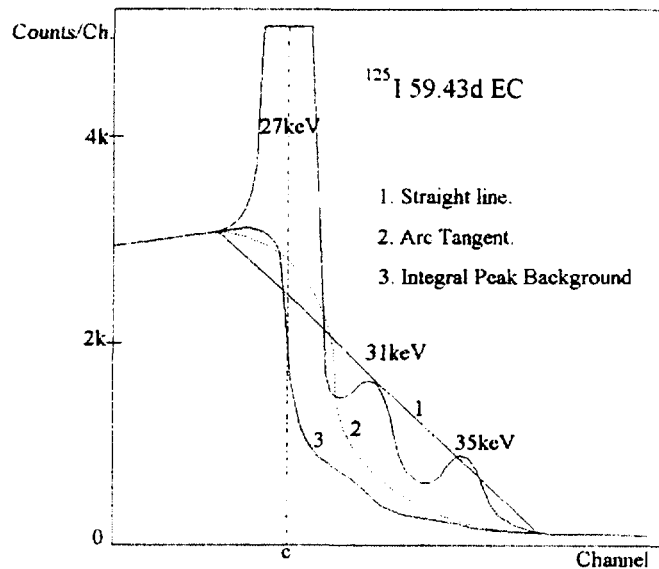


FIG. 2. Comparison of several baseline functions

The principle of the technique is described as below:

- (1) The peak causes the baseline step.
- (2) The baseline step height depends on the peak height and the peak energy. At the same energy the step is proportional to the net peak area of the peak. In the case of multiplets, for example, the stronger peak causes a larger step baseline.
- (3) From items 1 and 2 we can make an important inference: the change of the baseline per channel under a peak(s) is proportional to the net count of the relevant channel, that is:

$$dH = \frac{(A_i - B_i) * H_i}{S} \quad (4)$$

where  $dH$  is the change of the baseline,

$H_t$  is the total step height,

$A_i$  is the count in channel  $i$ ,

$B_i$  is the baseline in channel  $i$ .

$S$  is the net peak area of the peak(s) in the peak region, that is:

$$S = \sum_{i=l}^r (A_i - B_i) \quad (5)$$

where  $l$  and  $r$  are the left and right limits of the peak region, respectively.

The equations (4) and (5) are available for both singlet and multiplet. The slope of the baseline plateau before the peak is usually not zero, and after the peak the baseline is also slanting. We need to design a continuous baseline curve in the whole spectra region, that means at the peak left and right limit the integral baseline under the peak should be equal to the baseline outside the peak, and the slopes should be identical. We can find a baseline region out of the left or the right side, as shown in Fig.1 we can fit out a straight line in each continuum region:

$$y_1 = a_1 + b_1 * x \quad (\text{left side}) \quad (6)$$

$$y_2 = a_2 + b_2 * x \quad (\text{right side}) \quad (7)$$

Extending the straight lines to the center of the peak(s), we can get the total step amount:

$$H_t = a_1 + b_1 * c - a_2 - b_2 * c \quad (8)$$

Where  $c$  is the center of the peak(s), it may be expressed as:

$$c = \frac{\sum_{i=l}^r [(A_i - B_i) * i]}{\sum_{i=l}^r (A_i - B_i)} \quad (9)$$

Thus, we can express the background under the peak as:

$$B_i = a_1 + b_1 * i - \frac{H_t}{S} * \left[ \left\{ \sum_{k=l}^i (A_k - B_k) \right\} - \frac{A_i - B_i}{2} \right] \quad (10)$$

Of course,  $dH$ ,  $B_i$ ,  $c$  and  $H_t$  are interrelated each other, but not arbitrary. The initial  $B_i$  in a region is assumed by equations (6) and (7). The final values for  $B_i$  are obtained iteratively by using appropriate computer techniques. In detail the final values for  $B_i$  are obtained after following steps:

- (1) To find a baseline region out of the left or the right side and fit out a straight line for each of these baseline regions as equations (6) and (7), assuming the peak(s) top as the center for the peak(s).
- (2) To extend the straight lines (6) and (7) to the center of the peak(s), the initial  $B_i$  can be obtained.

- (3) Calculate the area of the peak according to equation (5).
- (4) According to equation (9), get the center of the peak(s).
- (5) To get new values of  $B_i$  according to equation (10).
- (6) To repeat steps 2 to 5, until all the parameters converged.

The convergence of the parameters is rather fast, only after 3-5 loops the calculation could be finished. Using this technique we can subtract the baseline before resolving multiplet, thus the parameters are decreased for resolving multiplet, so it can accelerate the data processing. It is more important that this technique can result in an acceptable baseline under both singlet and multiplet.

#### 8.4. EXPERIMENTAL PEAK SHAPE

For getting a better fitting we do not try to increase the parameter number of the analytical peak shapes, instead it is replaced with a numerical method, hereafter called *experimental peak shape*, to perform the multiplet fitting. The experimental peak shape is different from traditional analytical ones at following points:

We use a set of data to replace the traditional analytical peak shape function, the set of data was got from an experimental spectrum:

$$P_j = \frac{A_i - B_i}{S} \quad P_j = \sum_{i=k}^l (F_{ij} * P_i) \quad (11)$$

where  $P_j$  is the distribution factor of the peak in channel  $j$  (in experimental peak shape library) or channel  $i$  (in the spectrum), and  $j = i - \text{left-limit}$ .

$A_i$  is the counts in channel  $i$ .

$B_i$  is the baseline in channel  $i$ .

$S$  is the net peak area, got by equation (5).

A peak shape may be well described with 64 points of the data, meanwhile the peak center  $x_0$ , the peak width  $\sigma$  and peak energy  $E$  are also saved in the library as parameters. Then we can use the experimental peak shapes to fit the peaks in any other spectra, in which the peaks have different center  $x_0'$ , width  $\sigma'$  and area  $S$ , the experimental peak shape will be projected on the spectrum to be fitted. The projection shift depends on the peak centre  $x_0$  and  $x_0'$ , the projection amplification is calculated from peak width  $\sigma$  and  $\sigma'$ , peak height depends on the peak area  $S$ . The projection can be expressed as following:

$$P_j = \sum_{i=k}^l (F_{ij} * P_i) \quad (12)$$

where  $P_j$  is the distribution factor in channel  $j$  in the spectrum to be fitted.

$P_i$  is the distribution factor in channel  $i$  in the experimental peak shape library.

$F_{ij}$  is the conversion factor.

$k$  and  $l$  are the channels, on which the left and right limits of channel  $j$  are projected.

The accurate projection points are at  $x_1$  and  $x_2$ . The conversion factor can be calculated as follows and shown in Fig. 3:

$$F_{ij} = \begin{matrix} 1-[x_1-i] & \text{for } i=k \\ 1 & \text{for } k < I < 1 \\ x_2-i & \text{for } i=l \end{matrix} \quad (13)$$

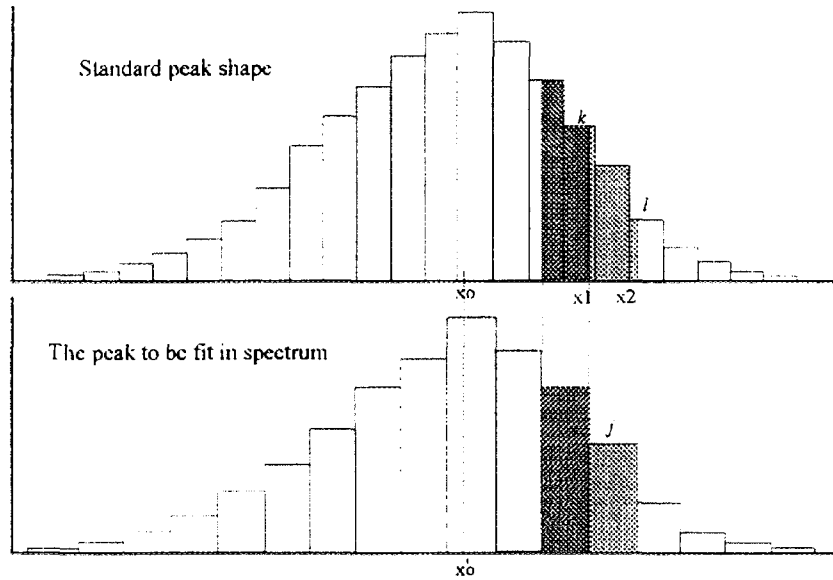


FIG. 3. The projection of the experimental peak shape onto spectrum.

The non-linear least square fitting is required to calculate the differential of peak shape, while traditionally this is performed by the analytical expression, here in the experimental peak shape it is done by the numerical method:

$$\frac{\partial f(x_0, \sigma, x)}{\partial x_0} = \frac{f(x_0 + \Delta x_0, \sigma, x) - f(x_0, \sigma, x)}{\Delta x_0} \quad (14)$$

$$\frac{\partial f(x_0, \sigma, x)}{\partial \sigma} = \frac{f(x_0, \sigma + \Delta \sigma, x) - f(x_0, \sigma, x)}{\Delta \sigma} \quad (15)$$

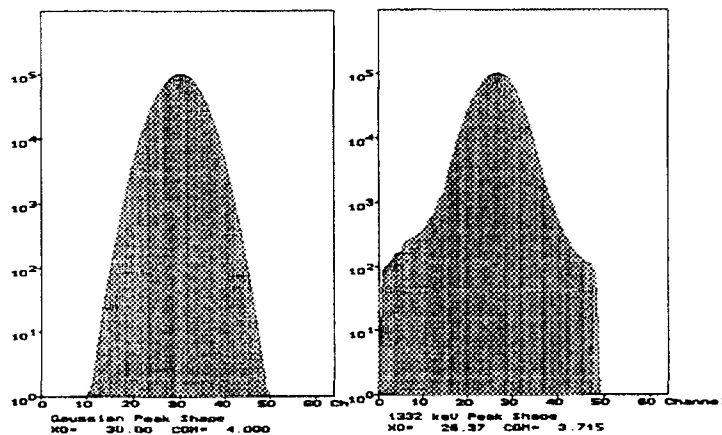


FIG. 4. The comparison between experimental peak shape and Gaussian peak shape.

The experimental peak shape has following advantages:

- The experimental peak shape is much similar to the peak shapes of the spectrum to be processed, because they are obtained from the same detector, so the fitting will be the best one if the experimental peak shape is accurate enough extracted.
- Only 3 parameters are needed to be fitted; they are: peak's centre, width and area. Much less than those needed when using analytical peak shape functions.
- The calculation of the experimental peak shape is much easier than the one for an analytical expression; the formal is just some simpler mathematical calculations.

Summing up above 3 points, we can say that the experimental peak shape can get a better and faster fit, and the result is much accurate. Figure 5 is an example of using experimental peak shape to fit multiplet. By the experimental peak shape, very much complex and overlapped multiplets, peaks with tails and non-symmetry peaks can be satisfactorily processed. In addition it does not increase any additional fitting parameters.

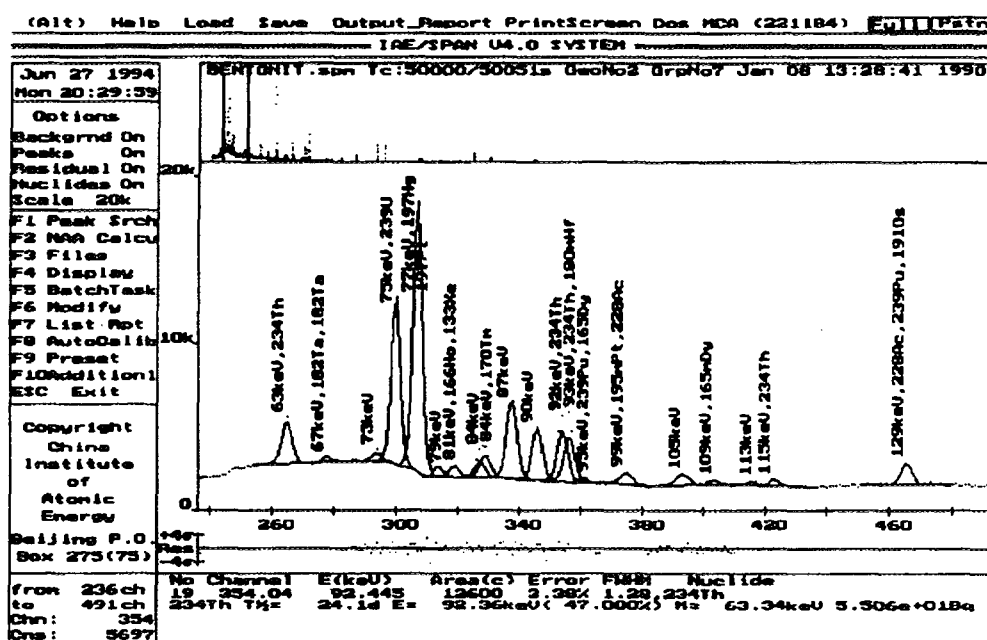


FIG. 5. An example of resolving multiplet with experimental peak shape.

## 8.5. THE KNOW-HOW IN PROCESSING X RAY SPECTRUM

The X ray spectrum is quite different from the  $\gamma$  ray spectrum in which the peaks are much more complex and overlapped. In X ray spectrometry some peaks are very close to each other, they can not be resolved one by one even with any mathematical methods. Moreover, if they could be resolved, the results would have a large inaccuracy. Because a lot of peaks jam up in the X ray spectrum, sometimes it is difficult to automatically find the peaks and the background regions, so some special methods have been developed in the software SPAN/XRF for X ray spectrum.

### 8.5.1. Preset peak position using the data in X ray data library

When the peaks are very crowded in X ray spectrum, to find every peak in the spectrum is difficult by normal peak searching program. Fortunately the elements in the X ray spectrum are not too many, and they usually have been known, or they could be assumed, so we can build up a sub-library, in which the known or assumed elements are included. According to the energy region of the spectrum section and the X ray energy in sub-library, all the possible peaks could be preset. Then the spectra can be fitted taking in consideration the preset peaks. If there is no peak at the preset position, the peak area should be near to zero and it could be deleted by the program. If there is a peak in the spectrum, but no relevant X ray line in the sub-library, the peak is called no-named peak, on which just mark an energy value without X ray and element name. If large residues are found after fitting the spectrum, that may be due to shortage of an element in the sub-library. Fig.6 is an example using the presetting method to analyse X ray spectrum.

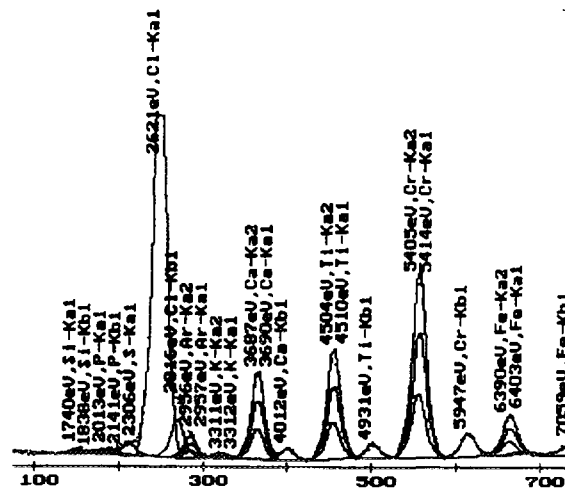


FIG. 6. An example using the presetting method to analyze X ray spectrum.

### 8.5.2. Complex peak shape

For some X rays in spectrum, their correspondent energies are very closed to each other, making it very difficult to resolved by mathematical method. If these X rays are of the same element, usually it is not necessary to resolve them, they can be processed as a complex peak. The complex peak can be expressed as following:

$$f_m(x_0, \sigma, x) = \sum [\Psi_i \varepsilon_i f_i(x_{0i}, \sigma, x)] / Y_0 \quad (16)$$

where  $f_m(x_0, s)$  is the complex peak,

$\Psi_i$  is the emission probability of X ray  $i$ ,

$\varepsilon_i$  is the detection efficiency of X ray  $i$ ,

$f_i(x_{oi}, \sigma, x)$  is the mono-energy peak shape function of X ray  $i$ ,

$x_{oi}$  is the centre of the peak of X ray  $i$ , which is calculated from X ray data library,

$\sigma$  is the peak width of the mono-energy peak, it needs to be fit, calibration value is used as the initial.

$$\Psi_0 = \sum \Psi_i * \varepsilon_i, \text{ is the normalization factor.}$$

Figure 7 is an example of using complex peak shape, in which 15 X rays peaks have been synthesized into 5 complex peaks for processing easily.

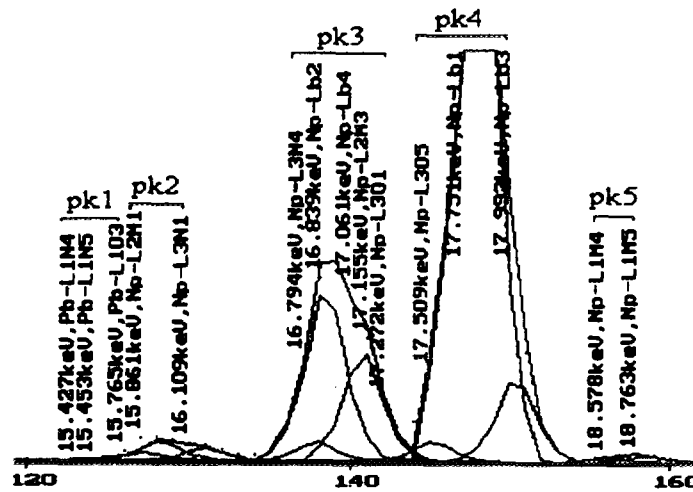


FIG. 7. An example using complex peak shape.

### 8.5.3. Manual setting of baseline region

The software SPAN analysing  $\gamma$  ray spectra finds the spectrum baseline automatically. But for X ray spectrum this performance is usually not successful due to the large amount of peaks. In order to resolve this problem, a method to set the baseline region was developed in X ray spectrum software SPAN/XRF, by which the spectrum could be processed satisfactorily.

### 8.6. THE OTHER CHARACTERISTICS OF SOFTWARE SPAN AND SPAN/XRF

Good software not only should possess accurately the spectrum, but also be convenient to use. A lot of auxiliary functions have been designed in the software SPAN and SPAN/XRF, including files management (load, save and convert), report output (peak analysis report, isotope report, neutron activation analysis report), detector calibration (energy, efficiency and FWHM calibration), library editing (nuclear data library, elements of interest and standard reference material), spectrum (original data, background, peaks and residual) and curves (calibration curves and peak shapes) displaying. Now some distinguished features are described here.

### 8.6.1. Good-looking and useful graphical capabilities

After processing the spectra, the analysis results: including baseline, peaks and residuals, and original spectrum data; are displayed on screen in different colours. The energy and relevant nuclide are marked on the top of each peak, so the analysis results are clearly seen at a glance. Several convenient possibilities were implemented in the software, by which the user can change the content and view of it; for example, fast and slow cursor movements, jumps from peak to peaks, window movements and different spectrum scales.

Furthermore the energy, FWHM and efficiency calibration curves; and the standard peak shapes can also be displayed on the screen. Screen capture capability has been implemented into the software so a spectra plotting can be pasted into a file or printed (black and white or coloured) into a plotter or printer.

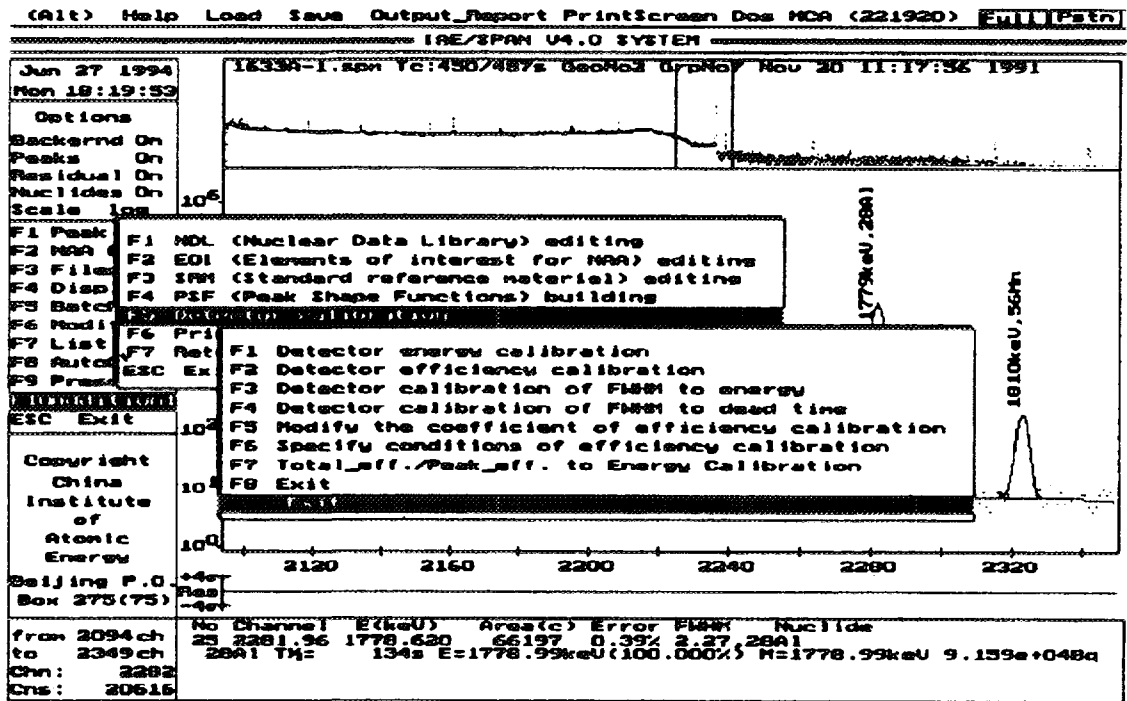


FIG. 8. The pop menus of the SPAN software.

### 8.6.2. Pop menu and mouse control

The software is operated by menu options and mouse (see Fig.8); so its operation is rather easy and without the necessity for reading the user's manual.

### 8.6.3. Batch mode operation

The software can operate in batch modes, meaning it can process several spectra (84) without the direct intervention of the user. After editing a batch sequence for a task, the spectra can be processed automatically with the corresponding analysis reports. Of course the batch mode operation can be interrupted or exited manually.

### 8.6.4. Easy energy calibration and efficiency calibration

A large  $\gamma$  ray data library (obtained from IAEA TECDOC-564[7]) and an X ray data library (from IAEA-TECDOC-619[8] and others) are included in the software SPAN and SPAN/XRF, respectively.

The energy and efficiency calibrations are easy to perform in these software. They are based on the data in the library and on the analysis results, only a few operations are required for the calibrations. For example only a few nuclides need to be entered for energy calibration, all the data are retrieved from software's library and the analysis results. The efficiency calibration is also rather easy, only the nuclide radioactivity, the decay time and spectrum file name are required to be entered. Then the selection of the user's choice peaks for this calibration. The efficiency calibration is performed using quadratic spline function on the two logarithmic coordinates (efficiency and energy). The calibration is shown in the screen, see Fig.9, which could be printed as well.

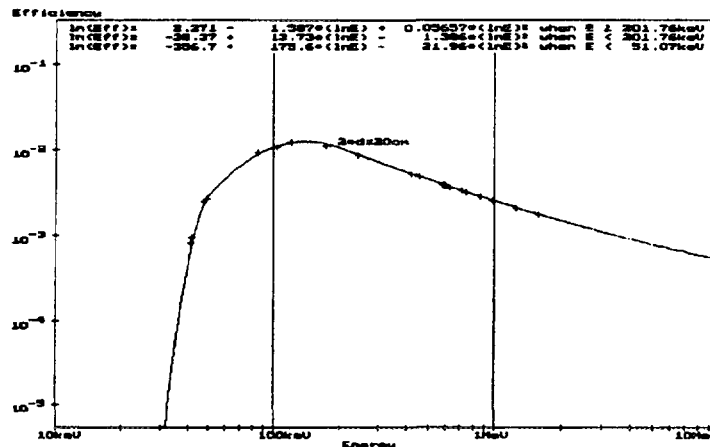


FIG. 9. Efficiency calibration curve of an HPGe detector

## 8.7. CONCLUSIONS

The software packages SPAN and SPAN/XRF use different approaches like "experimental peak shape", "integral background" and "complex peak shape" among others, with which the spectra can be processed quickly and accurately. The software SPAN is useful in neutron activation analysis, isotope identification, and environment radioactivity monitoring, as well. The software SPAN/XRF is used for X ray fluorescence analysis. Practice has proved that the techniques used in the software are successful and the analysis results are satisfactory.



- [1] S.I. NAJAFI, T. KIKINDAI, J. Radioanal. Chem. **68** (1982) 127–134.
- [2] W. WESTMEIER, Nucl. Instr. Meth. **180** (1981) 205–210.
- [3] G. W. PHILLIPS, K.W. MARLOW, Nucl. Instr. Meth. **137** (1976) 525.
- [4] J. KERN, Nucl. Instr. Meth. **180** (1981) 205–210.
- [5] W. WATZIG, "Computer in Activation Analysis Ray Spectroscopy", in Proc. American Nuclear Society Topical Conf. Mayaguez, Puerto Rico, 1978, US Department of Energy (1978) 150–156.
- [6] WANG LI-YU, Sci. Tech. At. En. **20** (1987) 436–439 (in Chinese).
- [7] INTERNATIONAL ATOMIC ENERGY AGENCY, Practical Aspects of Operating A Neutron Activation Analysis Laboratory, IAEA-TECDOC-564, Vienna (1990).
- [8] H.D. LEMMEL, et al., in X-ray and Gamma-ray Standards for Detector Calibration, IAEA-TECDOC-619, IAEA, Vienna (1991).
- [9] WANG LI-YU, Sci. Tech. At. En. **21** 2 (1987) 263–267 (in Chinese).
- [10] WANG LI-YU, Nuclear electronics and detector Technology **6** 6 (1986) 356 (in Chinese).
- [11] SHUNJI GOTO, Nucl. Instr. Meth. **A333** (1993) 452.
- [12] L.A. MCNELLES, J.L. CAMPBELL, Nucl. Instr. Meth. **127** (1975) 73.
- [13] Y. WATANABE, T. KUBOZOE, Nucl. Instr. Meth. **B17** (1986) 81.
- [14] M.C. LEPY, J. PLAGNARD, J. MOREL, Nucl. Instr. Meth. **A339** (1994) 241.

## **9. A PROCEDURE FOR INCORPORATING GAMMA RAY ATTENUATION CORRECTIONS INTO GERMANIUM EFFICIENCY CALIBRATIONS<sup>13</sup>**

### 9.1. SUMMARY

Quantification of radionuclide concentrations by gamma ray spectrometry is often complicated by the need to make self-absorption corrections. These corrections become especially important when the matrix composition or density of the calibration source is different from the samples that are being analyzed. At our laboratory attenuation corrections are being done by means of a computer program. Here a brief explanation of it is presented.

### 9.2. DISCUSSION

At the Environmental Measurements Laboratory the tedium of determining attenuation corrections by direct measurement has been replaced by computer calculations. Attenuation corrections are computed and applied to the calibration data to obtain a matrix free and weightless set of efficiency versus energy data points. These data points are then adjusted using the attenuation corrections computed for the sample being analysed. This results in an efficiency calibration that matches both sample composition and density.

---

<sup>13</sup> Prepared by C.G. Sanderson. Environmental Measurements Laboratory, United States of America.